ACS APPLIED MATERIALS & INTERFACES

Research Article

www.acsami.org

Biofunctionalization of Ulvan Scaffolds for Bone Tissue Engineering

Mamoni Dash,*[,†] Sangram K. Samal,[†] Cristina Bartoli,[‡] Andrea Morelli,[‡] Philippe F. Smet,[§] Peter Dubruel,[†] and Federica Chiellini[‡]

[†]Polymer Chemistry & Biomaterials Research Group, Ghent University, Krijgslaan 281, S4-Bis, B-9000 Ghent, Belgium

[‡]Department of Chemistry & Industrial Chemistry, University of Pisa−UdR-INSTM, Via Vecchia Livornese, University of Pisa, Pisa 1291, Italy

[§]Lumilab, Department of Solid State Sciences, Ghent University, Krijgslaan 281, S1, 9000 Gent, Belgium

ABSTRACT: Photo-cross-linked ulvan scaffolds were designed with the aim to induce and support enzyme mediated formation of apatite minerals, in the absence of osteogenic growth factors. Scaffold formation with a desired geometry was investigated using chemically modified ulvan bearing radically polymerizable groups. Further bioactivity was incorporated by the use of alkaline phosphatase (ALP) induced minerals. Successful modification of UV cross-linked ulvan scaffolds was revealed by ^{1}H NMR. The presence of the mineral formation was evidenced by Raman spectroscopy and XRD techniques. Investigations of the morphology confirmed the homogeneous mineralization using ALP. The MC3T3 cell activity clearly showed that the mineralization of the biofunctionalized ulvan scaffolds was effective in improving the cellular activity.

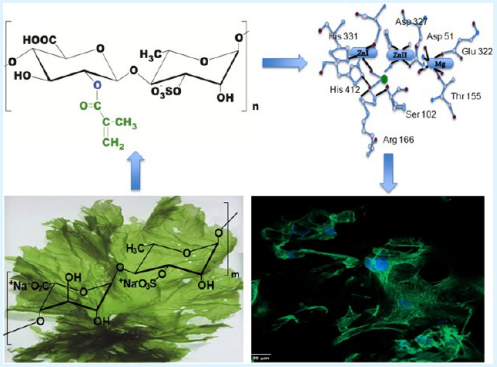

KEYWORDS: *ulvan, scaffolds, enzyme, mineral, tissue engineering*

INTRODUCTION

Bone tissue engineering is an emerging and promising approach for bone repair. A wide variety of advanced techniques are available to overcome the problems associated with bone repair, but all have their own advantages and disadvantages.[1] As a successful alternative, the use of synthetic bone grafts is an upcoming research topic, with notable benefits such as increased availability and reduced morbidity.[2,3] The engineering of such bone graft substitutes is usually composed of an artificial extracellular matrix as a scaffold, osteoblasts, and regulating factors that are capable of enhancing cell growth, differentiation, and mineralized bone tissue formation.[4] Among the above mentioned components, porous scaffolds have a crucial role in aiding cell seeding, proliferation, and new tissue formation in three dimensions (3D).[5] The scaffold acts as a 3D substrate for cells, and serves as a template for tissue regeneration. Scaffold material selection largely depends on the structural and biochemical properties, which would accelerate bone healing. Polymers have become a widely adopted choice as a scaffolding material.[6,7] Among several classes of polymers, polysaccharides, in particular, exhibit some excellent properties, which makes them the polymer group suitable for a wide range of medical applications.[8] In the present study, we have focused our research on biofunctionalization of a natural polysaccharide, namely ulvan, to develop resorbable graft materials for bone tissue engineering. In the context of this study, biofunctionalization is defined as the development of material to have biological function and/or stimulus and be biologically compatible.[9]

Ulvan is an anionic sulphated polysaccharide that is water-soluble and semi-crystalline in nature,[10] which can be obtained by extraction from the cell walls of the green seaweeds belonging to Ulvales (Ulva and Enteromorpha sp.).[11] The natural availability of ulvan represents a source of abundant and economic renewable resources[12] with minimal concerns regarding toxicity towards host organisms. The structure of ulvan consists of rare sugars namely sulphated rhamnose and iduronic acid in its backbone (Figure 1). In a previous study, by Morelli et al., ulvan was functionalized by incorporating radically polymerizable groups to enable UV cross-linking of hydrogels.[12] In the present study, these cross-linked ulvan hydrogels were biofunctionalized by employing the natural

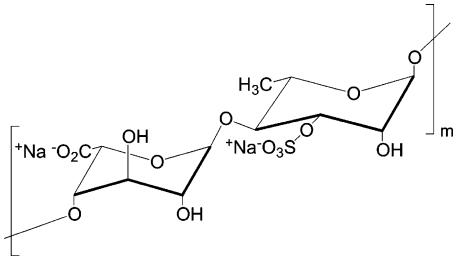

Figure 1. Chemical structure representing the main disaccharide repeating unit of ulvan, α-L-iduronic acid (1→4) α-L-Rha 3S→1.

Received: November 4, 2013
Accepted: February 4, 2014
Published: February 4, 2014

enzyme alkaline phosphatase (ALP) as mineralization inducer. Then the osteogenic cell activity on these scaffolds was evaluated. Mineralization is known to promote bioactivity, which is the formation of a chemical bond with neighboring bone tissues post implantation. Further advantages of mineralization include osteoblastic differentiation through increased stiffness[13] and enhanced binding of growth factors which stimulate bone healing.[14] ALP is secreted by osteoblasts and assists in liberating phosphates from organic phosphates, facilitating the precipitation of calcium phosphate crystals.[15] The applied strategy could lead to the understanding of the different stages of mineral formation when subjected to certain conditions in a polymer matrix in the form of a scaffold, to promote bone regeneration.

Mineralization and particularly enzymatic mineralization has been a topic of research interest over the last decade.[16,17] A number of investigations have been reported on matrices like chitosan,[18] fibrin[19,20,21] silk,[22] etc. In the present study, we have tried to investigate the role of enzymatic mineralization on polymeric structures bearing anionic groups. It has been observed that anionic proteins play a significant role in mineral phase deposition in natural bone and also affect mineralization in simulated body fluid (SBF).[23] The presence of anionic groups on a polymer backbone by incorporation or modification of the polymer backbone is a common approach for developing mineralized polymer scaffolds.[16,24] The choice for ulvan as the polymer matrix arises from these considerations, whereas the choice for UV polymerization for scaffold preparation is based on our previous investigation.[12]

EXPERIMENTAL SECTION

Materials. Bovine intestinal ALP (specific activity: ≥10 DEA units/mg, P7640) and calcium glycerol phosphate (50043) were obtained from Sigma (Sigma Aldrich, Belgium). Ulvan polysaccharide from *Ulva armoricana* was kindly supplied by CEVA (M_w = 60 KDa). 2-Hydroxy-4′-(2-hydroxy-ethoxy)-2-methyl-propiophenone (IRGACURE 2959) and methacrylic anhydride (MA) (Sigma-Aldrich) were used as received.

Pre-osteoblastic MC3T3-E1 cells were purchased from the American Type Culture Collection (CRL-2593). Cells were maintained and expanded in alpha modification minimum essential medium containing 10% fetal bovine serum, 100 U/mL penicillin, 0.1 mg/mL streptomycin and antimycotic agent (Invivogen) in humidified 5% CO_2 at 37 °C. Confluent MC3T3 cells at passage 25 were trypsinized (0.25% trypsin-EDTA), centrifuged and resuspended in complete medium and counted. Subsequently, 1×10^5 cells, initially dispersed in 20 μL of complete medium, were seeded onto the scaffolds in a 24 wells plate. After 3 h of incubation at 37 °C and in 5% CO_2, scaffolds were covered with 980 μl of complete medium. In order to assess the osteoblastic differentiation, 24 h after cells seeding the scaffolds were incubated in osteogenic medium supplemented with 10 mM β-glycerolphosphate and 0.3 mM ascorbic acid. Biological investigations were carried out at days 7 and 14 after seeding. The medium was replaced every 48 h. Cells grown on tissue culture plates were used as control.

Modification of Ulvan. In this study, ulvan was functionalized with methacrylate groups using methacrylic anhydride (MAA). Ulvan was reacted with methacrylic anhydride according to a published protocol of Morelli *et al.*[12] Briefly, to a solution containing Ulvan (1g, 0.0025 mol of repeating units) in deionized water (20 mL) MA (26.9 mL, 0.181 mol) was added carefully in order to avoid abrupt change of pH and temperature within the reaction mixture. An aqueous solution of NaOH 5N (1.12 molar ratio respect to MA) was then added dropwise to the reacting solution in order to maintain the pH between 7.5 and 8.0. The reacting solution was left stirring for 2 h at room temperature and further 24 h at 4 °C. The product was recovered as whitish flakes after precipitation into absolute ethanol (10:1 v/v), dialysis against water and freeze drying processing (24 h, −50 °C). Product yields typically ranged from 60 to 75%. The extent of conjugation of Ulvan to methacrylates was determined by ^{1}HNMR analysis as the mean number of methacryloyl groups linked to the repeating units of the polysaccharide (DS, Degree of Substitution). DS was calculated by ratio of the area of the peak relevant to the methyl group of methacrylate to the area of the signal of the rhamnose group of ulvan.

Polymer Scaffold Fabrication and Characterization. Ulvan-methacrylate (UMA) scaffolds were molded into small cylindrical shapes by equally distributing the aqueous solution containing the relevant macromer (5% w/v) and the cytocompatible UV photo-initiator IRGACURE 2959 (0.25% w/v) into each well of a 24 well microplate. The obtained viscous solutions were exposed to a UV light source (mercury vapor lamp, 8−10m W/cm^2, wavelength, 365 nm) for eight min and lyophilized at −50 °C for 24 h in order to obtain the dried scaffolds. The described solutions were characterized by ^{1}H NMR analysis before and after UV irradiation by using D_2O as solvent. ^{1}H NMR analysis was performed by using a Varian Gemini 200 MHz Fourier transform (FT) nuclear magnetic resonance (NMR) spectrometer. Spectra were recorded on 2% (w/v) solutions by using D_2O as solvent and processed by using Mestre software.

Mineralization of the Scaffolds. The scaffolds were incubated in a solution of ALP for 30 minutes. Three different concentrations of ALP were used in this study (5, 25, and 50 mg/mL). The ALP treated scaffolds of ulvan methacrylate will be denoted as UMA 5, UMA 25 and UMA 50 respectively. The ALP-soaked scaffolds (5×5 mm^2 for cell culture and 10×10 mm^2 for mechanical analysis) were subsequently incubated in a mineralization medium (5 and 10 mL, respectively) containing 0.1 M calcium glycerophosphate (aq) at 37 °C. The mineralization medium was refreshed every day. After 7 days of mineralization, scaffolds were rinsed thrice in Milli-Q water to remove residual calcium glycerophosphate and subjected to lyophilization after freezing at −20 °C.

Scaffold Morphology. Scanning Electron Microscopy (Hitachi S-3400N) was used to analyze the morphology of the scaffolds. Images were obtained in low vacuum mode (20 Pa) to avoid image distortions, using back scattered electrons. Elemental analysis was performed on a Peltier cooled dry EDS system (Thermo Scientific Noran System 7, energy resolution <125 eV).

Study of Scaffold Mass Increase. The mass increase of the scaffolds at different time points after the incubation in calcium glycerophosphate was calculated using previously established equation

$$\text{mass increase } (\%) = [(m_t - m_0)/m_0] \cdot 100$$

where m_t = the mass of scaffolds after incubation at time t and m_0 = the original mass of scaffolds before incubation and mineralization.

The final mass increase was calculated by using the same formula as above, but m_t is the dry mass of the scaffolds after mineralization.

Raman Spectroscopy. Fourier transform Raman (FT-Raman) spectra were performed on a NXR FT-Raman Module. The samples were pressed in a suitable gold coated sample holder and a laser power of 0.35 W was used to collect the scans;[25] 1500 scans were collected at a resolution of 4 cm^{-1}.

Thermal Analysis by Thermogravimetry (TGA). Thermogravimetric analyses were performed using a TA Instruments Series TA 2950 and results were analyzed using thermogravimetric analyzer software (Universal Analysis 2000). Sample weights of 9−13 mg were used and scanned at 10 °C min^{-1}. A temperature range between 30 and 900 °C under a 60 mL min^{-1} flow rate of nitrogen was used for the analysis.[25]

Crystal Structure Elucidation by X-ray Diffraction (XRD). XRD technique was used to investigate the crystallographic structure of the samples. A X-ray diffractometer with CuKα-radiation (PW 3710, 50 kV, 40 mA) was used. Samples were fixed to a position of 2.5° and scanning the detector between 5 and 40° 2θ with a counting time of 5 s/step and step-size of 0.01° 2θ.

Biological Investigations. *Cell Viability and Proliferation.* MC3T3-E1 cell viability and proliferation was assessed by direct cell

Scheme 1. Schematic Representation of UMA Synthesis

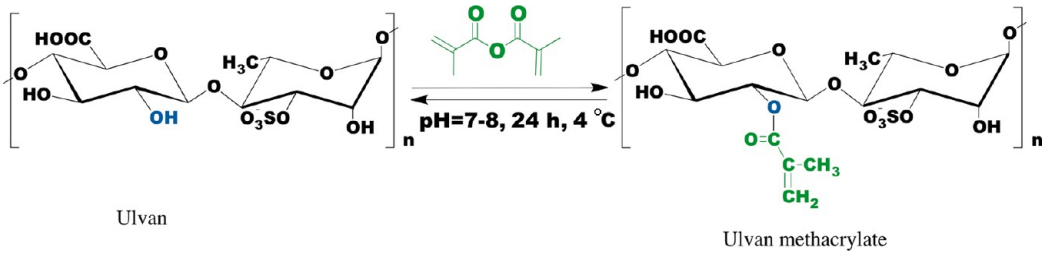

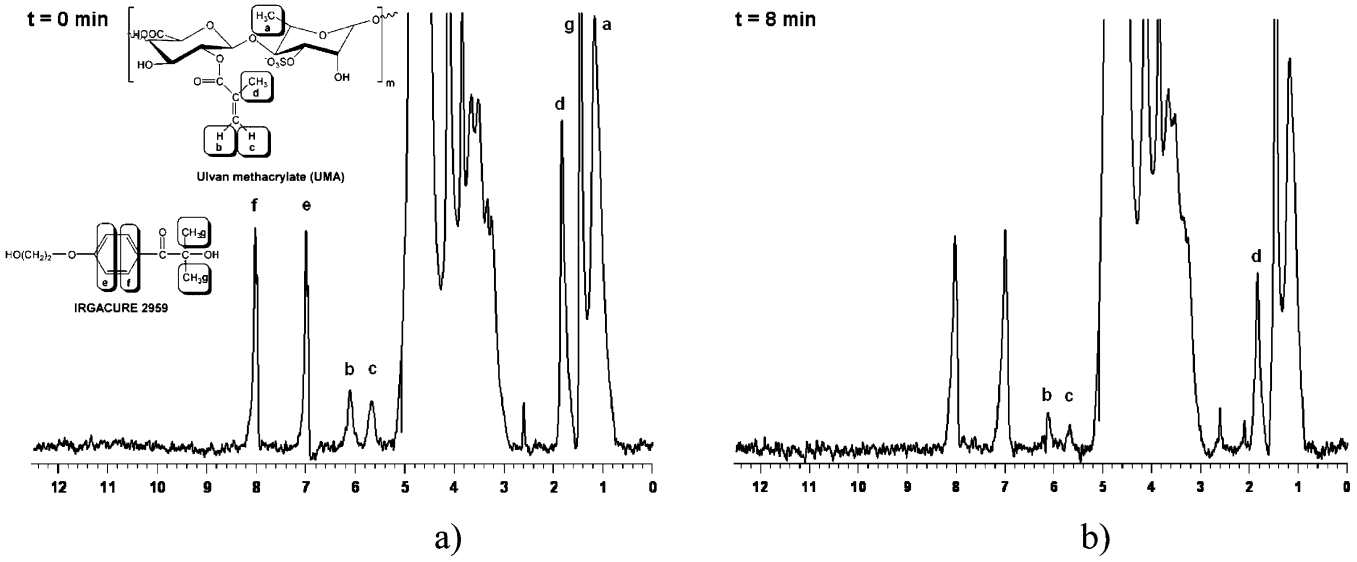

Figure 2. ^{1}HNMR spectra of (a) pristine solution of UMA and IRGACURE 2959 prior to UV cross-linking along with their relevant peak assignment (t = 0), (b) cross-linked UMA samples after 8 mins of UV exposure (t = 8).

counting using the vital dye trypan blue. Culture media was removed, scaffolds were washed twice with Dulbecco Phosphate Buffer Saline (DPBS) and then incubated with 600 μL of 0.25% trypsin solution (containing 1 mM EDTA) at 37 °C, 5% CO_2 for 15−20 min. After cells had detached, complete medium was added and the cells were stained by using trypan blue. Briefly, 0.4% trypan blue dye was mixed to the cell suspension and hemocytometer counting chamber was used to determine the number of viable and nonviable cells.

Alkaline Phosphatase (ALP) Activity. Alkaline phosphatase activity ALP was determined in culture using MC3T3-E1 cells grown onto the prepared scaffolds at day 7 according to previously established protocols.[26] Briefly, treated scaffolds were washed three times with DPBS, treated with lysis buffer, containing Triton X-100 (0.2%), magnesium chloride (5 mM) and trizma base (10 mM) at pH 10, for 15 min at 4 °C. Cell lysate was centrifuged for 15 min at 10 000 rpm at 4 °C. 20 μL of supernatant were collected and incubated with p-nitrophenyl phosphate at 37 °C for 30 min. The reaction was stopped by the addition of 2M NaOH. The absorbance at 405 nm was measured with a UV-vis spectrophotometer. The amount of ALP was calculated against a standard curve and normalized to the total proteins. ALP activity was expressed as nanomoles (nmol) of *p*-nitrophenol produced per minute.

Total Protein. Cellular protein content was measured with a BCA protein assay kit (Pierce, USA) to determine the cellular protein content following a protocol of St-Pierre et al.[27] Cell lysate was incubated with bicinchoninic acid solution for 2 h at 37 °C and the absorbance were measured at 565 nm in a microplate reader. A standard curve using bovine serum albumin was used to generate a standard curve.

Quantification of Total Collagen Production. Quantification of total collagen produced by cells seeded on scaffolds was carried out at day 7. The detailed protocol has been described by Gazzari et al.[26] Briefly, medium was removed and samples were rinsed in DPBS. Scaffolds were then incubated for 1 h with a solution of Direct Red 80 dye (Sigma) prepared in picric acid (0.1%). Dye excess was removed by washing the samples with 10 mM HCl. Bound stain solution was obtained with the incubation 0.1 N NaOH. The absorbance of the dye was read at 540 nm. Known concentrations of collagen type I, filmed on glass slides, were prepared and used for the standard curve. The films were then fixed and treated as the samples.[28]

Confocal Laser Scanning Microscopy (CLSM). CLSM investigation was performed to evaluate the morphology of the osteoblasts grown on scaffolds on day 14 of the culture according to a protocol by Gazzari et al.[26] Briefly, scaffolds with cells were fixed for 1 h in 3.8% paraformaldehyde in PBS and permeabilized with 0.2% Triton X-100 for 10 min.

The Nikon Eclipse TE2000 inverted microscope (Nikon) and 60X oil immersion objective was employed for sample investigation. Argon Ion Laser (488 nm emission) and a laser diode (405 nm) were used to excite FITC and DAPI fluorophores respectively. Images were captured with Nikon EZ-C1 software applying identical instrumental settings for each sample, and were further processed with the GIMP (GNU Free Software Foundation) image manipulation software and merged with Nikon ACT-2U software.

Statistical Analysis. Data were obtained from triplicate samples and are presented as mean ± standard deviation. Statistical comparison was performed using one-way analysis of variance (ANOVA), and significance was defined at $p < 0.05$ (*) and $p < 0.001$ (**).

RESULTS AND DISCUSSION

Chemical Modification and Biofunctionalization of Ulvan. In accordance with an established protocol,[12] the schematic representation of the methacrylation reaction of ulvan is shown in Scheme 1. The pH of the solution was

dx.doi.org/10.1021/am404912c | ACS Appl. Mater. Interfaces 2014, 6, 3211−3218

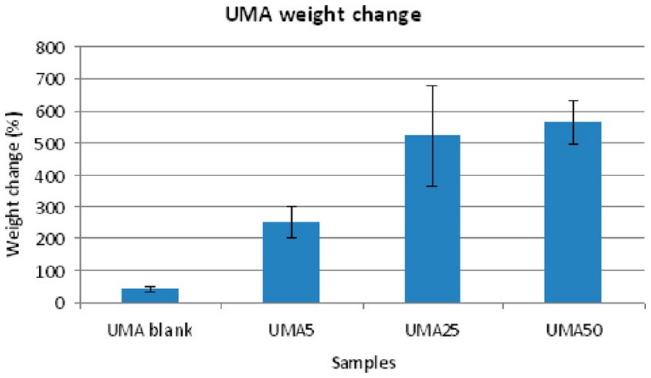

Figure 3. Increase in dry mass after 7 days of mineralization of UMA.

maintained slightly basic in order to neutralize the forming methacrylic acid thus promoting the conjugation between Ulvan and the methacryloyl group and reduce the extent of hydrolysis of the just formed ester group (Scheme 1). The temperature of reaction was controlled to limit the formation of side-products due to hydrolysis reactions and thermally induced polymerization of the large excess of methacrylate groups present in the reaction mixture. The successful preparation of UMA was confirmed spectroscopically by ^{1}HNMR (Figure 2) and FT-IR analysis (data not shown).

UMA scaffolds were covalently cross-linked by radical process through photo-induced polymerization of the methacryloyl groups present within the structure of the UMA macromers. The detailed data relevant to the ^{1}HNMR characterization of the UV photo-cross-linked UMA scaffolds have been reported by Morelli et al.[12] The results indicated that the UV exposure successfully induced cross-linking within the macromer chains by triggering the covalent reaction between the methacryloyl groups.[12] Although the yield of cross-linking was not found to be complete even after ten minutes of irradiation, a rapid exposure of the macromer solution to UV lamp was sufficient to obtain stable scaffolds. The scaffolds prepared for biomineralization were UV exposed for eight minutes and the extent of cross-linking was characterized by ^{1}HNMR analysis (Figure 2).

Table 1. Atomic Percentage of Calcium, Oxygen, Phosphorus, and Sulfur on the Mineralized Scaffolds

sample	calcium	oxygen	phosphorus	sulfur
UMA blank	11.9	76.7	10.2	1.3
UMA 5	22.0	61.1	15.2	1.7
UMA 25	13.6	74.3	12.0	0.1
UMA 50	15.9	72.5	11.4	0.3

Table 2. Ca/P Ratio of the Mineralized Scaffolds

sample	Ca/P ratio
UMA blank	1.16
UMA 5	1.44
UMA 25	1.31
UMA 50	1.39

The vinyl protons are indicated by the peaks b and c. The peak d is indicative of the methyl of the methacryloyl groups. At the end of the UV exposure, the intensity of the peaks b, c and d were found to decrease with respect to those of the photoinitiator (Figure 2b) taken as standard. The intensity of the signals was measured by the area under each peak, which is a good measure of the relative ratios of the different kinds of protons. This confirms the successful covalent reaction between the methacryloyl groups of the macromer (Figure 2).[12] Although the conversion was not complete as attested by the residual presence of the vinyl peaks b and c, the obtained hydrogels were nevertheless stable.

The use of UV light for the preparation of the scaffolds allowed for a rapid and straightforward procedure without the use of conventional catalysts and time consuming protocols, which are usually required for covalent cross-linking. The

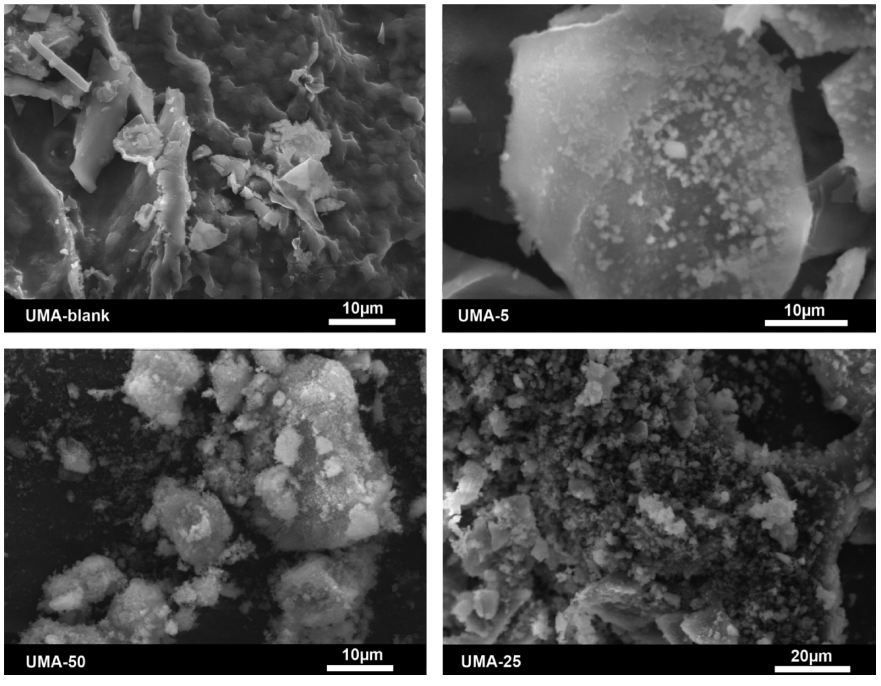

Figure 4. SEM images of UMA scaffolds; increasing concentration of ALP are represented in a clockwise direction.

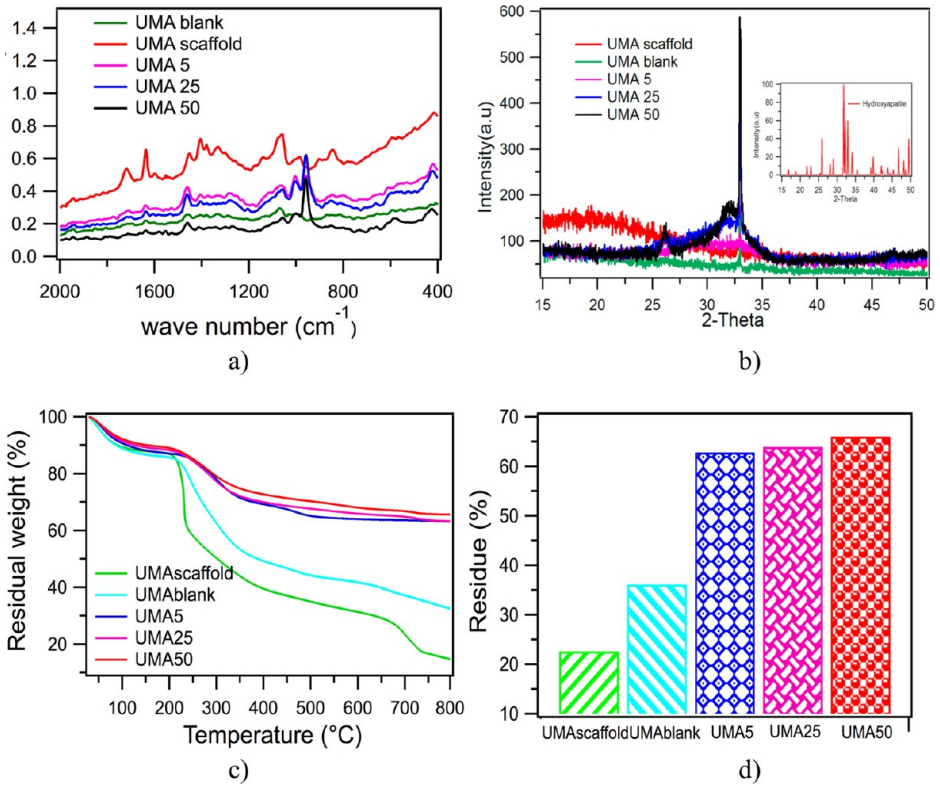

Figure 5. (a) Raman spectra of ulvan scaffolds mineralized in the presence of different ALP concentrations, (b) X-ray diffraction patterns of mineralized ulvan scaffolds with different ALP concentrations (the blank scaffold was unmineralized), (c) TGA curves of native and mineralized ulvan scaffolds, (d) mineral residue content in the presence of different ALP concentrations.

presence of carboxyl ester groups in the cross-links would guarantee the degradability of the polymer network at physiological conditions.

The process of freeze drying is expected to introduce porosity to the hydrogels. These pores are utilized for nucleation of mineral crystals induced by ALP. ALP is known for its importance in hard tissue formation. Among various hypotheses, this metalloenzyme is considered as a mineralization promotor that enhances the concentration of inorganic phosphate at the site and decreases the concentration of extracellular pyrophosphate, which is considered to be an inhibitor of mineral formation.[29] ALP assists in liberating phosphates from the calcium glycerol phosphate medium, facilitating the precipitation of calcium phosphate crystals in the pores of the ulvan scaffolds.

Physical-chemical Characterizations of Biomineralized Scaffolds. The dry mass percentages of the mineralized ulvan scaffolds, which represent the gel weight percentage not consisting of water, are shown in Figure 3. Dry mass percentage increased upon raising the ALP concentration from 0 to 50 mg mL^{-1} after the studied period of 7 days. An approximate six fold increase in the UMA scaffold weight was observed after 1 week of mineralization with the highest concentration of ALP.

After scaffold mineralization with different ALP concentrations, the morphology of the deposits was analyzed with SEM (Figure 4) and their chemical composition was determined using EDS. The surface of the UMA scaffolds was covered with crystals upon treatment with ALP. This was clearly observed upon comparison with the blank scaffold, which had no crystal formation on its surface. The crystals had the appearance of agglomerates of globular structures. After ALP assisted mineralization, the crystals on the scaffold surface were analysed with EDS using the spot analysis mode. The EDS analysis indicated a Ca/P ratio of around 1.16 in the blank scaffold, because of the remaining calcium glycerol phosphate (with a Ca/P ratio of 1 in the starting medium). The presence of sulphur is originating from the polymer matrix. EDS analysis of the blank substrate indicated oxygen (76.7 at%) as the main heavy ($Z > 7$) constituent (Table 1). Carbon was not considered in the analysis, partly because of contributions from the black carbon tape used to support the samples. Calcium and phosphorus were observed in all cases of mineralized samples (Table 2), and the atomic ratio had increased compared to the blank to 1.3−1.45, which is getting close to the expected Ca/P ratio of 5/3 in apatite.

The results of the Raman spectroscopy analyses revealed a strong peak at 958 cm^{-1} characteristic for the P−O stretching mode ($\nu 1$) of the phosphate group (Figure 5 a). The peak is not observed in both the blank and the scaffold of UMA, but appeared clearly in the mineralized scaffolds. The intensity of the peak was directly related to the concentration of the ALP used.

The X-ray diffractograms of the scaffolds mineralized for different durations are shown in Figure 5b. All the patterns showed a broad reflection peak around 32° 2θ. In addition, a peak was observed for UMA 25 and UMA 50 at 26° 2θ. UMA 5 did not show any peak similar to the blank sample. The positions of the broader peaks are in line with the expected positions of hydroxylapatite (HA) as can be observed from the reference pattern of HA (see insert in Figure 5b). The broadness of the peaks could be explained by the formation of small nanosized crystallites, instead of micrometer-scale single crystals.

dx.doi.org/10.1021/am404912c | ACS Appl. Mater. Interfaces 2014, 6, 3211−3218

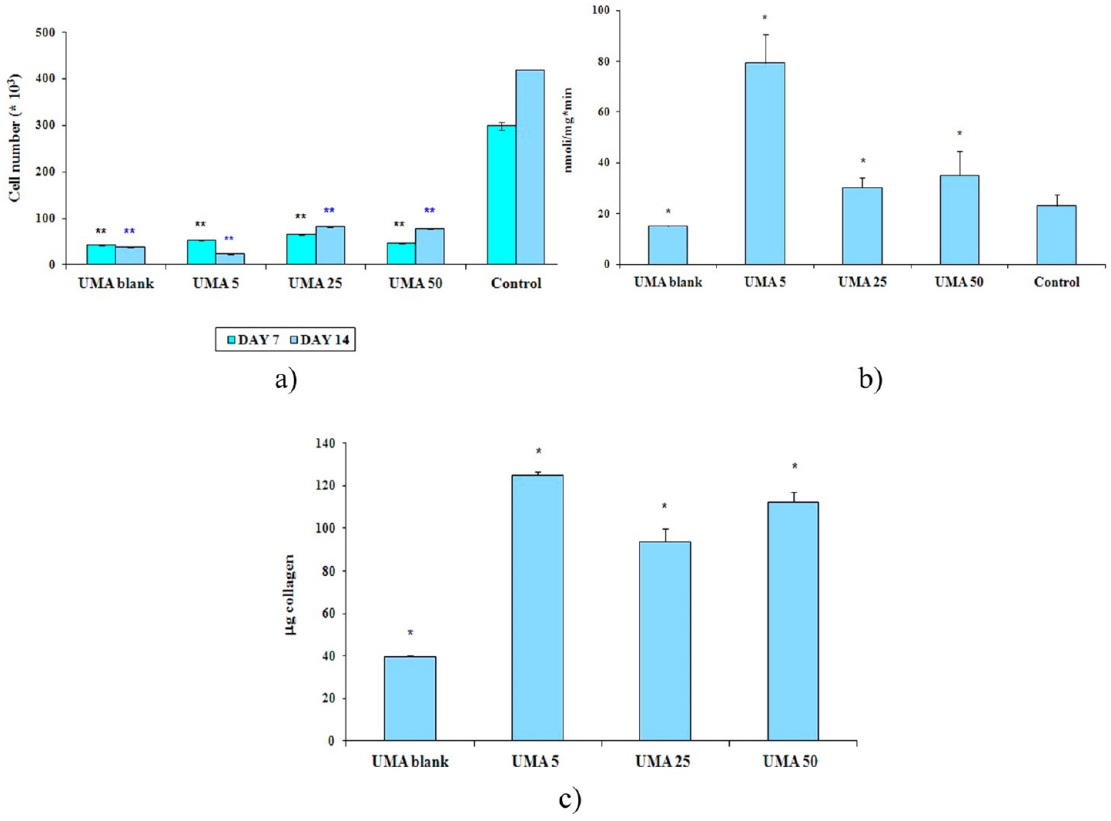

Figure 6. (a) Cell proliferation of MC3T3 × 10^{-1} cultured on ulvan methacrylate scaffolds. ** (black) Significant at $p < 0.001$ compared to the control at day 7. ** (blue) Significant at $p < 0.001$ with respect to control at day 14. (b) Alkaline phosphatase activity of MC3T3 × 10^{-1} cells grown on ulvan methacrylate scaffolds. *Significant at $p < 0.05$ with comparison to control at day 7. (c) Collagen production obtained from MC3T3 × 10^{-1} cells cultured onto UMA scaffolds. * Significant at $p < 0.05$ between different samples at day 7.

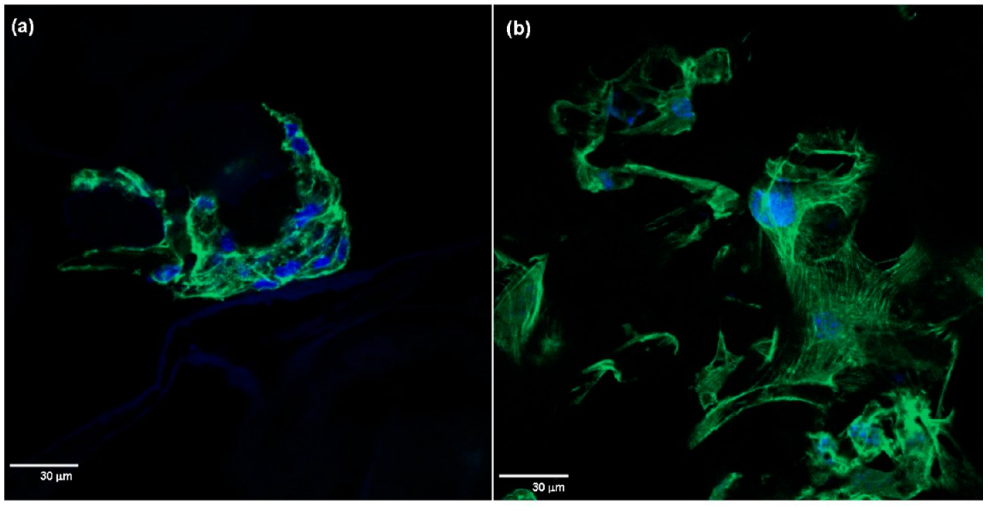

Figure 7. CLSM micrographs of MC3T3 × 10^{-1} cells cultured on (a) UMA blank scaffolds and on (b) UMA 5 scaffolds at 20× magnification.

The stability of the mineral crystals on the polymer scaffold was analysed by TGA. The TGA traces of the native and the mineralized ulvan scaffolds are shown in Figure 5c. All the traces show a continuous weight loss up to 600 °C. The first weight loss step was observed in the temperature range 30−150 °C, followed by a continuous weight loss ranging from 200 to 450 °C. The mineral residue of the mineralized and unmineralized scaffolds are presented in Figure 5d, which indicate a clear increase in the mineral content after mineralization.

In Vitro Biological Evaluation of Scaffolds Bioactivity. Cell viability and proliferation was determined by counting the number of viable MC3T3-E1 cells grown on the prepared scaffolds using the trypan blue dye exclusion assay. MC3T3-E1 cultured on all typologies of UMA scaffolds highlighted appreciable values of cell proliferation, even if they were significantly lower with respect to the cells cultured on TCPS at all time points (Figure 6a). In particular, at day 14 of culture, cell proliferation on non enzymatically treated UMA sample (UMA blank) was significantly lower with respect to those

observed on UMA 25 and UMA 50 samples. Furthermore, UMA 25 and UMA 50 were able to support a slow but increasing cell proliferation within two weeks of culture. Differentiation of MC3T3-E1 cells, grown on the prepared constructs, into mature osteoblasts was investigated by measuring ALP activity as an early differentiation marker.[30] Figure 6b shows the ALP activity of MC3T3-E1 cells grown on UMA scaffolds. At day 7 the ALP values of cells grown on enzymatically treated samples were significantly higher with respect to the control and to the untreated sample (UMA blank) ($p < 0.05$). In particular, UMA 5 sample showed the highest ALP value although displaying a limited cell number.

The observed results in terms of ALP activity suggest an early beginning of the differentiation process towards an osteoblastic phenotype for the cells grown onto the enzymatically treated scaffolds. As reported by the literature, osteoblast differentiation is commonly characterized by a diminished cell proliferation and increased activity of ALP.[30] The synthesis of collagen correlates with the expression of osteoblast phenotype in MC3T3-E1 cells.[31] MC3T3-E1 cells grown on enzymatically treated UMA scaffolds exhibited values of collagen production (Figure 6c) significantly higher with respect to the untreated sample (UMA blank) ($p < 0.05$). The results showed that the enzymatically treated UMA scaffolds induced MC3T3-E1 cells to produce collagen. This confirms the differentiation towards an osteoblast phenotype as highlighted also by the ALP investigations.

The influence of the different scaffolds on cell morphology and cytoskeleton organization was investigated by using confocal laser scanning microscopy. Cells were stained for F-actin and nuclei with FITC-phalloidin and DAPI respectively. After 14 days of culture, microscopic observations revealed a low number of adherent MC3T3 cells on the surface of the UMA blank and UMA 5 scaffolds, confirming the cell proliferation data (Figure 7a). However, cells grown on UMA 5 showed a polygonal morphology with an actin structure similar to the osteoblast phenotype (Figure 7b). This result is in agreement with the data related to ALP activity and collagen production and suggests the suitability of the UMA 5 scaffold to induce an osteogenic differentiation of MC3T3-E1 cells.

CONCLUSIONS

The present study demonstrated the feasibility of producing photo-cross-linked polymeric ulvan scaffolds that are enzymatically treated for calcium phosphate deposition. Photoreactive functional groups were introduced onto ulvan to prepare cross-linked scaffolds. The cross-linked ulvan scaffolds were treated with ALP and mineral formation was successfully induced. It was clearly observed that the ulvan scaffolds were homogeneously mineralized at ambient temperature as indicated by SEM. The XRD and FTIR analyses confirmed the phase structure of the formed minerals, which contained apatite. The different concentrations of the enzyme indicated difference in morphology and Ca/P ratio. The mineralized scaffolds were found to be non-toxic and the presence of the minerals, improved the osteogenic cells' activity on the scaffolds. A potential application of such scaffolds could be their use as resorbable bone graft substitutes, for which it is imperative to optimize the resorption rate compared to the mechanical properties, which are of lesser importance. The two important parameters when designing such substitutes are the geometry and the chemistry of the polymers used. With this study, we investigated scaffold formation with a desired geometry using chemically modified ulvan and further incorporated bioactivity via the use of ALP induced minerals. A comparison of such scaffolds with the extracellular matrix is the subject of future investigations.

AUTHOR INFORMATION

Corresponding Author

*E-mail: mamonidash@gmail.com. Tel.: +3292644508. Fax: +3292644972.

Notes

The authors declare no competing financial interest.

ACKNOWLEDGMENTS

The group of Prof. Pascal Van Der Voort and Dr. Timothy E. L. Douglas are highly acknowledged for their help.

REFERENCES

(1) Kolk, A.; Handschel, J.; Drescher, W.; Rothamel, D.; Kloss, F.; Blessmann, M.; Heiland, M.; Wolff, K.-D.; Smeets, R. *J. Craniomaxillofac Surg.* **2012**, *40*, 706−718.
(2) Bose, S.; Roy, M.; Bandyopadhyay, A. *Trends Biotechnol.* **2012**, *30*, 546−554.
(3) Moore, W. R.; Graves, S. E.; Bain, G. I. *ANZ J. Surg.* **2001**, *71*, 354−361.
(4) Wang, X. H.; Shi, S.; Guo, G.; Fu, S. Z.; Fan, M.; Luo, F.; Zhao, X.; Wei, Y. Q.; Qian, Z. Y. *J. Biomater. Sci., Polym. Ed.* **2011**, *22*, 1917−1929.
(5) Jithendra, P.; Rajam, A. M.; Kalaivani, T.; Mandal, A. B.; Rose, C. *ACS Appl. Mater. Interfaces* **2013**, *5*, 7291−7298.
(6) Nair, L. S.; Laurencin, C. T. *Prog. Polym. Sci.* **2007**, *32*, 762−798.
(7) Hunt, N.; Grover, L. *Biotechnol Lett* **2010**, *32*, 733−742.
(8) Puppi, D.; Chiellini, F.; Piras, A. M.; Chiellini, E. *Prog. Polym. Sci.* **2010**, *35*, 403−440.
(9) Das, M.; Bandyopadhyay, D.; Singh, R. P.; Harde, H.; Kumar, S.; Jain, S. *J. Mater. Chem.* **2012**, *22*, 24652−24667.
(10) Alves, A.; Pinho, E. D.; Neves, N. M.; Sousa, R. A.; Reis, R. L. *Int. J. Pharm.* **2012**, *426*, 76−81.
(11) Robic, A.; Gaillard, C.; Sassi, J.-F.; Lerat, Y.; Lahaye, M. *Biopolymers* **2009**, *91*, 652−664.
(12) Morelli, A.; Chiellini, F. *Macromol. Chem. Phys.* **2010**, *211*, 821−832.
(13) Engler, A. J.; Sen, S.; Sweeney, H. L.; Discher, D. E. *Cell* **2006**, *126*, 677−689.
(14) Ruhé, P. Q.; Boerman, O. C.; Russel, F. G. M.; Spauwen, P. H. M.; Mikos, A. G.; Jansen, J. A. *J. Controlled Release* **2005**, *106*, 162−171.
(15) Omelon, S. J.; Grynpas, M. D. *Chem. Rev.* **2008**, *108*, 4694−4715.
(16) Mikos, A.G.; Kretlow, J. D. *Tissue Eng.* **2007**, *13*, 927−938.
(17) Gkioni, K.; Leeuwenburgh, S. C. G.; Douglas, T. E. L.; Mikos, A.G.; Jansen, J.A. *Tissue Eng., Part B* **2010**, *6*, 577−585.
(18) Douglas, T. E. L.; Skwarczynska, A.; Modrzejewska, Z.; Balcaen, L.; Schaubroeck, D.; Lycke, S.; Vanhaecke, F.; Vandenabeele, P.; Dubruel, P.; Jansen, J. A.; Leeuwenburgh, S. C. G. *Int. J. Biol. Macromol.* **2013**, *56*, 122−132.
(19) Douglas, T. E. L.; Gassling, V.; Declercq, H. A.; Purcz, N.; Pamula, E.; Haugen, H. J.; Chasan, S.; de Mulder, E. L. W.; Jansen, J. A.; Leeuwenburgh, S. C. G. *J. Biomed. Mater. Res., Part A* **2012**, *100A*, 1335−1346.
(20) Gassling, V.; Douglas, T. E. L.; Purcz, N.; Schaubroeck, D.; Balcaen, L.; Bliznuk, V.; Declercq, H. A.; Vanhaecke, F.; Dubruel, P. *Biomed. Mater.* **2013**, *8*, 055001.
(21) Douglas, T. E. L.; Messersmith, P. B.; Chasan, S.; Mikos, A. G.; de Mulder, E. L. W.; Dickson, G.; Schaubroeck, D.; Balcaen, L.; Vanhaecke, F.; Dubruel, P.; Jansen, J. A.; Leeuwenburgh, S. C. G. *Macromol. Biosci.* **2012**, *12*, 1077−1089.

(22) Samal, S.K.; Dash, M.; Declercq, H. A.; Gheysens, T.; Dendooven, J.; VanDerVoort, P.; Cornelissen, R.; Dubruel, P.; Kaplan, D. L. *Macromol. Biosci.* **2014**, *14*, 10.1002/mabi.201300513
(23) Olszta, M. J.; Cheng, X.; Jee, S. S.; Kumar, R.; Kim, Y.-Y.; Kaufman, M. J.; Douglas, E. P.; Gower, L. B. *Mater. Sci. Eng., R* **2007**, *58*, 77−116.
(24) Palmer, L. C.; Newcomb, C. J.; Kaltz, S. R.; Spoerke, E. D.; Stupp, S. I. *Chem. Rev.* **2008**, *108*, 4754−4783.
(25) Samal, S. K.; Dash, M.; Chiellini, F.; Kaplan, D. L.; Chiellini, E. *Acta Biomater.* **2013**, *9*, 8192−8199.
(26) Gazzarri, M.; Bartoli, C.; Mota, C.; Puppi, D.; Dinucci, D.; Volpi, S.; Chiellini, F. *J. Bioact. Compat. Polym.* **2013**, *28*, 492−507.
(27) St-Pierre, J.-P.; Gauthier, M.; Lefebvre, L.-P.; Tabrizian, M. *Biomaterials* **2005**, *26*, 7319−7328.
(28) Junqueira, L. C. U.; Bignolas, G.; Brentani, R. R. *Anal. Biochem.* **1979**, *94*, 96−99.
(29) Golub, E. E.; Boesze-Battaglia, K. *Curr. Opin. Orthop.* **2007**, *18*, 444−448.
(30) Quarles, L. D.; Yohay, D. A.; Lever, L. W.; Caton, R.; Wenstrup, R. J. *J. Bone Miner. Res.* **1992**, *7*, 683−692.
(31) Franceschi, R. T.; Iyer, B. S. *J. Bone Miner. Res.* **1992**, *7*, 235−246.